



Journal of Mechanics of Materials and Structures

**LONGITUDINAL SHEAR BEHAVIOR OF COMPOSITES WITH
UNIDIRECTIONAL PERIODIC NANOFIBERS OF
SOME REGULAR POLYGONAL SHAPES**

Hai-Bing Yang, Cheng Huang, Chuan-bin Yu and Cun-Fa Gao

Volume 13, No. 2

March 2018



LONGITUDINAL SHEAR BEHAVIOR OF COMPOSITES WITH UNIDIRECTIONAL PERIODIC NANOFIBERS OF SOME REGULAR POLYGONAL SHAPES

HAI-BING YANG, CHENG HUANG, CHUAN-BIN YU AND CUN-FA GAO

Based on the Gurtin–Murdoch interface model, a complex variable-based approach is presented to study the longitudinal shear behavior of composites containing unidirectional periodic nanofibers. For intuitive demonstration, numerical results of the interfacial stress concentration and the effective (longitudinal) shear moduli are calculated for composites containing circular and (approximately) regular polygonal fibers. Graphic illustrations show that the interaction among periodic nanofibers can be neglected in the prediction of the interfacial stress field when the volume fraction of the fibers is less than 7%. For reasonably given interface parameters, fiber volume fraction and fiber size, the composite containing periodic circular fibers can achieve a lowest sensitivity of effective shear moduli to the interface effect among all the aforementioned fiber shapes. Moreover, we show that if the fibers are much harder than the surrounding matrix (for example, the shear modulus of the fibers exceeds twice that of the matrix), the corresponding interface effect can make only negligible contributions to the effective longitudinal shear moduli of the composites.

1. Introduction

Based on the concept of surface stress associated with the excess free energy of a material surface, Gurtin, Murdoch and coworkers [[Gurtin and Murdoch 1975](#); [1978](#); [Gurtin et al. 1998](#)] developed a general continuum-based mechanical model, known as the Gurtin–Murdoch model, for a material surface/interface with residual tension and elasticity. In the past two decades, the Gurtin–Murdoch model has contributed greatly to the investigations of mechanical behavior of composites containing nanoparticles or nanofibers. For example, in the context of the Gurtin–Murdoch model, the stress state in the vicinity of spherical nanoparticles and circular/elliptical nanofibers embedded in a foreign matrix was studied, respectively, in [[Sharma et al. 2003](#); [Lim et al. 2006](#); [Tian and Rajapakse 2007](#); [Luo and Wang 2009](#); [Mogilevskaya et al. 2008](#); [Dai et al. 2016d](#); [2018](#)], while the effective moduli of composites with spherical nanoparticles and circular nanofibers were examined in [[Duan et al. 2005](#); [Chen et al. 2007](#); [Mogilevskaya et al. 2010](#); [Yvonnet et al. 2008](#); [Dai et al. 2016c](#); [2016b](#); [2017](#)], respectively.

Based on the Gurtin–Murdoch model, present work aims to establish an alternative numerical procedure to determine the longitudinal shear properties of composites containing periodic polygon-shaped nanofibers. The work is motivated by the fact that there are only few available methods besides the finite element method for the prediction of the elastic behavior of composites containing periodic nanofibers, and particularly is inspired by the paper [[Dai et al. 2016c](#)], involving periodic circular nanofibers. Based on the methodology in that paper, however, the extension of circular inclusions to noncircular inclusions

Keywords: Gurtin–Murdoch model, nanofiber, periodic fibers, interface effect, effective modulus.

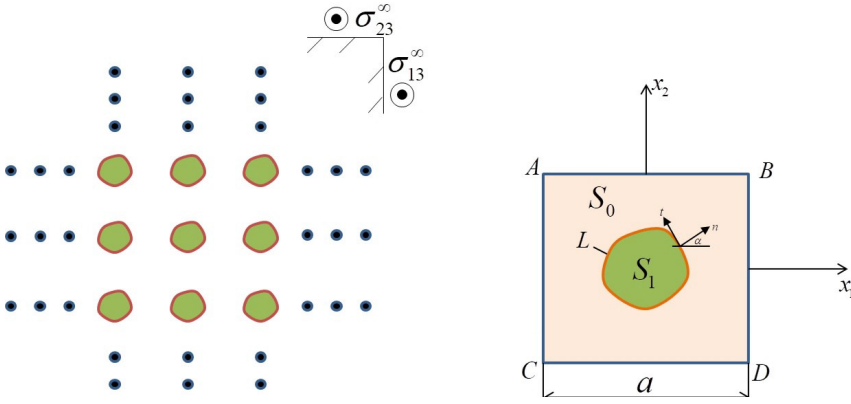


Figure 1. Left: an elastic matrix containing periodic array of nanofibers. Right: a representative square unit cell.

(e.g., polygonal inclusions) is difficult. In fact, as in [Dai et al. 2016c], it is relatively easy to extract the equations with respect to the unknown coefficients since the complex potentials of the circular inclusions are represented by the Taylor series (which is simple in form), but for polygonal inclusions it is usually difficult to do the same thing because the corresponding complex potentials can only be described by general Faber series which has a much more complicated form than the Taylor series. Consequently, it is still nontrivial to design an effective procedure with efficient numerical implementation to calculate the stress field for polygonal inclusions.

This paper is organized as follows. The boundary-value problem for composites with periodic polygon-shaped nanofibers under uniform remote longitudinal shear loadings is formulated in Section 2, and its series solution is established in Section 3. Several numerical examples are presented in Section 4 for validating our solution and illustrating the mechanical behavior of the corresponding composites. Finally, the main remarks constitute Section 5.

2. Problem description

As shown in Figure 1a, an elastic matrix (shear modulus G_0) containing a periodic array of unidirectional (approximately) polygonal nanofibers (shear modulus G_1) under uniform remote antiplane shear loadings σ_{13}^∞ and σ_{23}^∞ is considered. The influences of the nanofibers are described by the interface effect arising from the interface energies based on the Gurtin–Murdoch model [1975]. Here, to make the problem relatively tractable, we simply choose the representative unit cell (RUC), i.e., a square with the side length denoted by a (Figure 1b). For convenience, we denote the regions occupied by the matrix, the fiber and the interface between them, as S_0 , S_1 , and L , respectively. In particular, the indices (superscripts or subscripts) 0 and 1 are used to denote the physical quantities belonging to the matrix and fiber in the RUC, respectively.

According to the Gurtin–Murdoch mode, the elastic fields in the bulk region (S_0 , S_1) still satisfy the classical governing equations except for the stress discontinuity at the interfaces. In detail, the governing

equations for the out-of-plane displacement w and the antiplane shear stresses are given by

$$\frac{\partial^2 w^{(i)}}{\partial x_1^2} + \frac{\partial^2 w^{(i)}}{\partial x_2^2} = 0, \quad i = 0, 1, \quad (1)$$

$$\sigma_{13}^{(i)} = G_i \frac{\partial w^{(i)}}{\partial x_1}, \quad \sigma_{23}^{(i)} = G_i \frac{\partial w^{(i)}}{\partial x_2}, \quad i = 0, 1, \quad (2)$$

while the boundary condition on the interface are described as

$$w^{(1)} - w^{(0)} = 0, \quad \sigma_{n3}^{(1)} - \sigma_{n3}^{(0)} = G_s \frac{d^2 w^{(1)}}{ds^2} \quad \text{on } L, \quad (3)$$

where σ_{n3} is the shear traction on the interface L with n denoting the direction of outward normal to L (see [Figure 1b](#)), G_s is the interface shear modulus, and ds denotes the arc length of an element of the curve L along its tangent.

In addition to the boundary condition (3) on L , the periodic boundary condition on the edge $ABCD$ of the RUC can be expressed as [\[Xia et al. 2003\]](#)

$$\left. \begin{aligned} w^{(0)}\left(\frac{1}{2}a, x_2\right) - w^{(0)}\left(-\frac{1}{2}a, x_2\right) &= \Delta_1 \\ w^{(0)}\left(x_1, \frac{1}{2}a\right) - w^{(0)}\left(x_1, -\frac{1}{2}a\right) &= \Delta_2 \end{aligned} \right\} \quad \forall |x_1|, |x_2| \leq \frac{1}{2}a, \quad (4)$$

$$\left. \begin{aligned} (dw^{(0)}/dx_2)|_{(x_1, a/2)} &= (dw^{(0)}/dx_2)|_{(x_1, -a/2)} \\ (dw^{(0)}/dx_1)|_{(a/2, x_2)} &= (dw^{(0)}/dx_1)|_{(-a/2, x_2)} \end{aligned} \right\} \quad \forall |x_1|, |x_2| \leq \frac{1}{2}a, \quad (5)$$

where Δ_1 and Δ_2 are the constant increments between displacements on the sides DB and CA as well as AB and CD , respectively (see [Figure 1b](#)). Furthermore, these two increments can be determined by equilibrium equation on the sides AB and DB :

$$\int_A^B \sigma_{23}^{(0)}\left(x_1, \frac{1}{2}a\right) \frac{dx_1}{a} = \sigma_{23}^\infty, \quad \int_D^B \sigma_{13}^{(0)}\left(\frac{1}{2}a, x_2\right) \frac{dx_2}{a} = \sigma_{21}^\infty. \quad (6)$$

3. Solution procedure

General solutions to (1) and (2) can be given in terms of two complex potentials $f_i(z)$ ($i = 0, 1$) as [\[Muskhelishvili 1975\]](#)

$$w^{(i)} = \text{Im} f_i(z), \quad i = 0, 1, \quad (7)$$

$$\sigma_{23}^{(i)} + I\sigma_{13}^{(i)} = G_i f_i'(z), \quad i = 0, 1, \quad (8)$$

with

$$z = x_1 + Ix_2, \quad (9)$$

where the symbol I denotes the imaginary unit. In addition, the shear traction σ_{n3} on the interface L can be written as [\[Luo and Wang 2009\]](#)

$$\sigma_{23}^{(i)} = G_i \text{Im}[f_i'(t)e^{I\alpha}], \quad t \in L, \quad i = 0, 1, \quad (10)$$

where α is the angle between the normal direction n and the positive x_1 axis (see Figure 1b). Thus, by (7) and (10), the condition (3) can be rewritten in the form as

$$\begin{aligned} \operatorname{Im} f_0(t) &= \operatorname{Im} f_1(t), \\ \operatorname{Re} f_0(t) - \gamma \operatorname{Re} f_1(t) - \gamma R \operatorname{Re}[f_1'(t)e^{I\alpha}] &= 0, \quad t \in L, \end{aligned} \tag{11}$$

with

$$\gamma = \frac{G_1}{G_0}, \quad \lambda = \frac{G_s}{G_0 R}. \tag{12}$$

In particular, the second equation in (11) comes from the integration of the second equation in (3) with respect to the arc length of L .

Using (7), conditions (4) and (5) can be rewritten as

$$\operatorname{Im} f_0(z^{DB}) - \operatorname{Im} f_0(z^{CA}) = \Delta_1, \quad \operatorname{Im} f_0(z^{AB}) - \operatorname{Im} f_0(z^{CD}) = \Delta_2, \tag{13}$$

$$\operatorname{Re} f_0'(z^{AB}) - \operatorname{Re} f_0'(z^{CD}) = 0, \quad \operatorname{Im} f_0'(z^{DB}) - \operatorname{Im} f_0'(z^{CA}) = 0, \tag{14}$$

where z^{AB} , z^{CD} , z^{DB} , and z^{CA} represent the points of uniform distribution located on the sides AB , CD , DB , and CA , respectively. Furthermore, the following relations should be satisfied:

$$z^{AB} = \overline{z^{CD}}, \quad z^{DB} = -\overline{z^{CA}}. \tag{15}$$

In addition, by using (8), the condition (6) becomes

$$\begin{aligned} \int_A^B \operatorname{Re} f_0'(z) \frac{dz}{a} &= \frac{\sigma_{23}^\infty}{G_0}, \\ \int_D^B \operatorname{Im} f_0'(z) \frac{dz}{a} &= I \frac{\sigma_{13}^\infty}{G_0}. \end{aligned} \tag{16}$$

Here, we introduce a conformal mapping which transforms the boundary L in the physical z -plane into a unit circle in the imaginary ξ -plane, as [Muskhelishvili 1975]

$$z = \omega(\xi) = R \left(\xi + \sum_{n=1}^{+\infty} t_n \xi^{-n} \right), \quad |\xi| \geq 1, \tag{17}$$

where R and t_n denote the constants determined by the overall size and shape of L . Subsequently, the complex function $f_1(z)$ in S_1 can be represented approximately via the following truncated Faber series as

$$f_1(z) = \sum_{j=1}^N a_j P_{1j}(z), \tag{18}$$

where $P_{1j}(z)$ is a Faber polynomial for the region S_1 and satisfies

$$P_{1j}(z) = \xi^j(z) + \sum_{n=1}^{\infty} \beta_{j,n} \xi^{-n}(z), \tag{19}$$

on L , where

$$\beta_{1,n} = t_n, \quad \beta_{j+1,n} = t_{j+n} + \beta_{j,n+1} + \sum_{i=1}^n t_{n-1} \beta_{j,i} - \sum_{i=1}^j t_{j-1} \beta_{i,n}, \quad j, n = 1, 2, \dots \quad (20)$$

In the above formulas (18)–(20), a_j ($j = 1, \dots, N$) are the unknown complex coefficients to be determined and t_n ($n = 1, 2, \dots$) are the constant coefficients of the mapping (17). Similarly, the complex function $f_0(z)$ in S_0 can be expressed in terms of the superposition principle as follows [Dai et al. 2016a]:

$$f_0(z) = \sum_{j=1}^N b_j \xi^{-j} + \sum_{j=1}^M c_j P_j(z), \quad (21)$$

with

$$P_{j+1}(z) = P_1(z)P_j(z) - \sum_{k=1}^{j-1} m_k P_{j-k}(z) - (j+1)m_j, \quad (j = 1, \dots, M-1),$$

$$P_1(z) = \frac{143z}{84a}, \quad m_k = \begin{cases} -\frac{1}{6} & k = 3, \\ \frac{1}{56} & k = 7, \\ 0 & k = \text{others}, \end{cases} \quad (22)$$

where b_j ($j = 1, \dots, N$) and c_j ($j = 1, \dots, M$) are the unknown complex coefficients to be determined, while $P_j(z)$ ($j = 1 \dots M$) is a Faber polynomials of an (approximate) square region.

Substituting the defined complex potentials (18) and (21) into the corresponding boundary conditions (Equations (11), (13), (14) and (16)) leads to the solutions of coefficients a_j ($j = 1, \dots, N$), b_j ($j = 1, \dots, N$), and c_j ($j = 1, \dots, M$) via the Fourier expansion method. In detail, a system of linear equations with respect to the unknown coefficients a_j ($j = 1, \dots, N$), b_j ($j = 1, \dots, N$) and c_j ($j = 1, \dots, M$) can be obtained by equating the corresponding coefficients on the two sides of equations on the internal interface L . On the external boundary $ABCD$, a collocation method is used by choosing K ($K \geq M/2$) collocation points equidistantly on each side to deal with the periodic boundary conditions (13) and (14), then a system of linear equations can be extracted with respect to the unknown coefficients b_j ($j = 1, \dots, N$) and c_j ($j = 1, \dots, M$). Using the method in [Dai et al. 2016c], all the unknown coefficients can be described by the two parameters Δ_1 and Δ_2 . In terms of the two mean stress conditions (see (16)), the two parameters Δ_1 and Δ_2 can be obtained uniquely, and then the coefficients a_j ($j = 1, \dots, N$), b_j ($j = 1, \dots, N$), and c_j ($j = 1, \dots, M$) are all determined. Once the actual complex potentials $f_i(z)$ ($i = 0, 1$) are found, the displacement and stress field in the entire RUC are obtained using (7) and (8).

In addition, referring to the present Cartesian coordinate system, the effective longitudinal shear moduli (denoted by G_{1313} , G_{1323} , G_{2313} , and G_{2323}) of the composite can be defined based on the obtained stress and displacement as

$$\begin{bmatrix} G_{1313} & G_{1323} \\ G_{2313} & G_{2323} \end{bmatrix} \cdot \begin{bmatrix} \Delta_1/a \\ \Delta_2/a \end{bmatrix} = \begin{bmatrix} \sigma_{13}^\infty \\ \sigma_{23}^\infty \end{bmatrix}. \quad (23)$$

It is noteworthy that determination of all the effective shear moduli involve considering two independent kinds of external loadings (for example, $\sigma_{13}^\infty \neq 0$, $\sigma_{23}^\infty = 0$ and $\sigma_{13}^\infty = 0$, $\sigma_{23}^\infty \neq 0$) and calculating the corresponding parameters Δ_1 and Δ_2 , respectively.

4. Numerical examples

In this section, we focus on the examples for circular nanofibers and regular polygonal nanofibers, in which corresponding mappings (17) are given approximately as [Muskhelishvili 1975]

$$\omega(\xi) = R\xi \quad (\text{circle}), \quad (24)$$

$$\omega(\xi) = R\left(\xi + \frac{1}{3}\xi^{-2}\right) \quad (\text{triangle}), \quad (25)$$

$$\omega(\xi) = R\left(\xi - \frac{1}{6}\xi^{-3}\right) \quad (\text{square1}), \quad (26)$$

$$\omega(\xi) = R\left(\xi + \frac{1}{6}\xi^{-3}\right) \quad (\text{square2}), \quad (27)$$

$$\omega(\xi) = R\left(\xi + \frac{1}{10}\xi^{-4}\right) \quad (\text{pentagon}), \quad (28)$$

$$\omega(\xi) = R\left(\xi + \frac{1}{15}\xi^{-5}\right) \quad (\text{hexagon}), \quad (29)$$

where R characterizes the radius or side length of corresponding fibers. It is worth noting that the maximum volume fraction of the fibers varies with the fiber shape. In particular, when R is prescribed within the nanoscale, the normalized interface parameter λ defined in (12) is usually of the order 10^{-2} to 10^{-1} [Ruud et al. 1993; Josell et al. 1999].

4.1. Resultant stress fields around interface. Here, we define the resultant shear stresses $\sigma^{(i)}$ ($i = 0, 1$) and σ^∞ as follows:

$$\sigma^{(i)} = \sqrt{\sigma_{13}^{(i)2} + \sigma_{23}^{(i)2}}, \quad i = 1, 2, \quad (30)$$

$$\sigma^\infty = \sqrt{\sigma_{13}^{\infty 2} + \sigma_{23}^{\infty 2}}. \quad (31)$$

Figures 2 and 3 show the resultant shear stresses around the variously shaped interface between fiber volume fraction (VF) for $\sigma_{13}^\infty = \sigma_{23}^\infty$, $\lambda = 0.12$. It can be seen from Figures 2 and 3 that the results for periodic fibers converge to those for a single fiber in an infinite plane (see the corresponding results in [Wang and Schiavone 2014]) as the volume fraction of the fibers decreases, roughly speaking, to 7%. This suggests that one can use the simpler model of a single fiber in an infinite plane to predict approximately the stress concentration around periodic fibers when the fiber volume fraction falls below 7%.

4.2. Effective shear moduli. From an extensive collection of our numerical examples for fibers of various shapes (including those defined in (24)–(29)), it is found from Figures 4 and 5 that the increment Δ_1 is always zero when $\sigma_{23}^\infty = 0$ while the increment Δ_2 is always zero when $\sigma_{13}^\infty = 0$. This suggests that the shear stress σ_{13}^∞ does not induce the shear strain in the x_2 - x_3 plane while the shear stress σ_{23}^∞ does not induce the shear strain in the x_1 - x_3 plane (here x_3 denotes the coordinate axis perpendicular to the x_1 - x_2 plane). That is to say, the minor effective shear moduli G_{1323} and G_{2313} are always zero, which implies that the effective longitudinal shear properties of the composite with periodic circular or regular polygonal fibers are almost orthotropic in terms of our present reference coordinate system. All

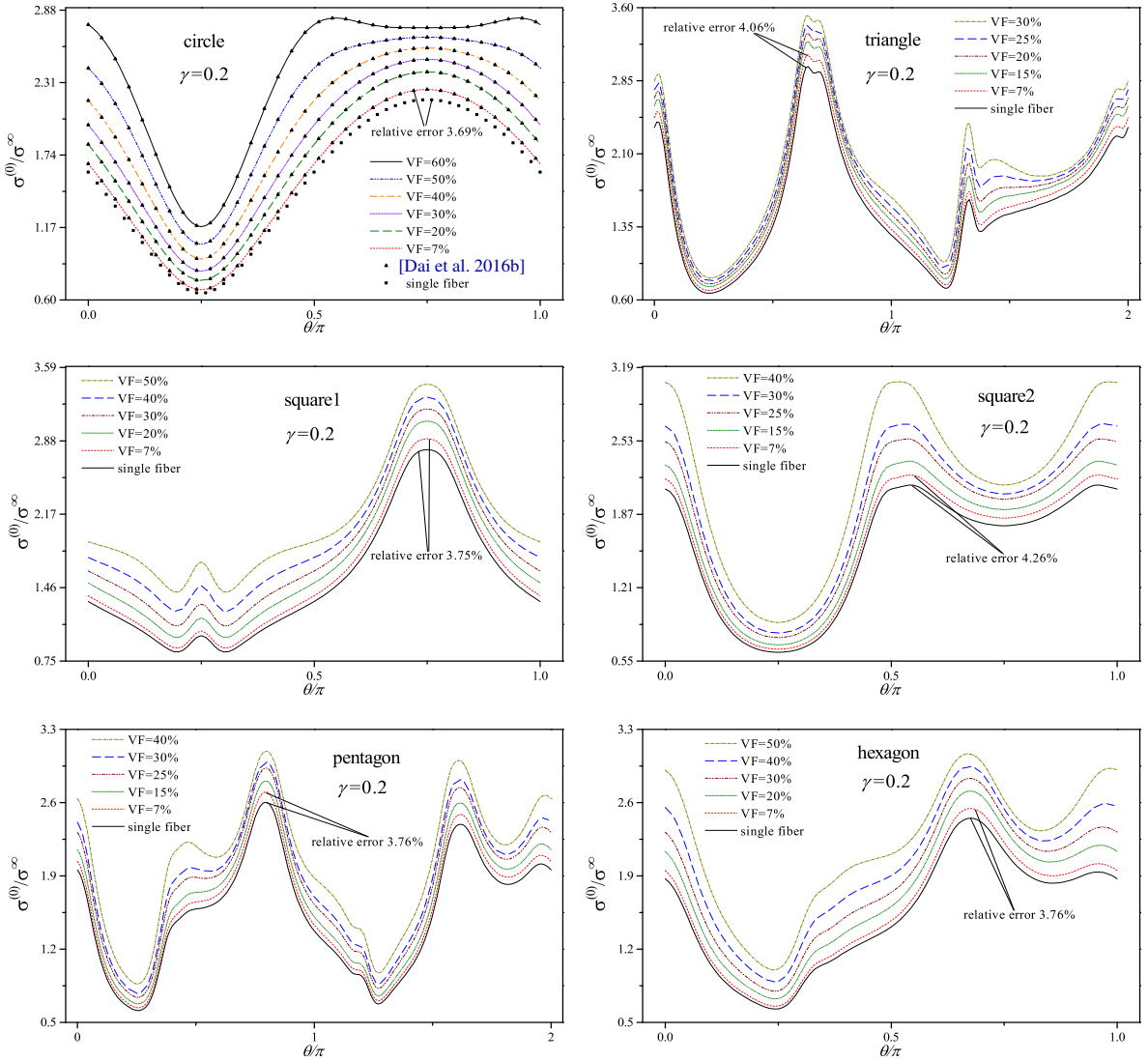


Figure 2. Resultant shear stresses around matrix on the interface between soft fiber and matrix. In each panel, the lowermost curve or dotted line shows single-fiber data from [Wang and Schiavone 2014]; remaining curves are reference data from [Dai et al. 2016c].

things considered, the zero values of these coupled shear moduli may be due to the perpendicularity in the direction of period.

In the remaining examples, one of the purposes is to study the influence of the shear modulus of the nanofibers on the effective longitudinal shear properties of the composite. To do this, however, requires that the interface shear modulus G_s not be treated as a fixed parameter when the shear modulus of the nanofibers changes since the interface shear modulus depends on not only the bulk properties of the matrix but also those of the nanofibers. Here, we treat the interface as the assembly of the surfaces of the matrix and nanofibers so that the interface shear modulus G_s is defined as the sum of the surface shear

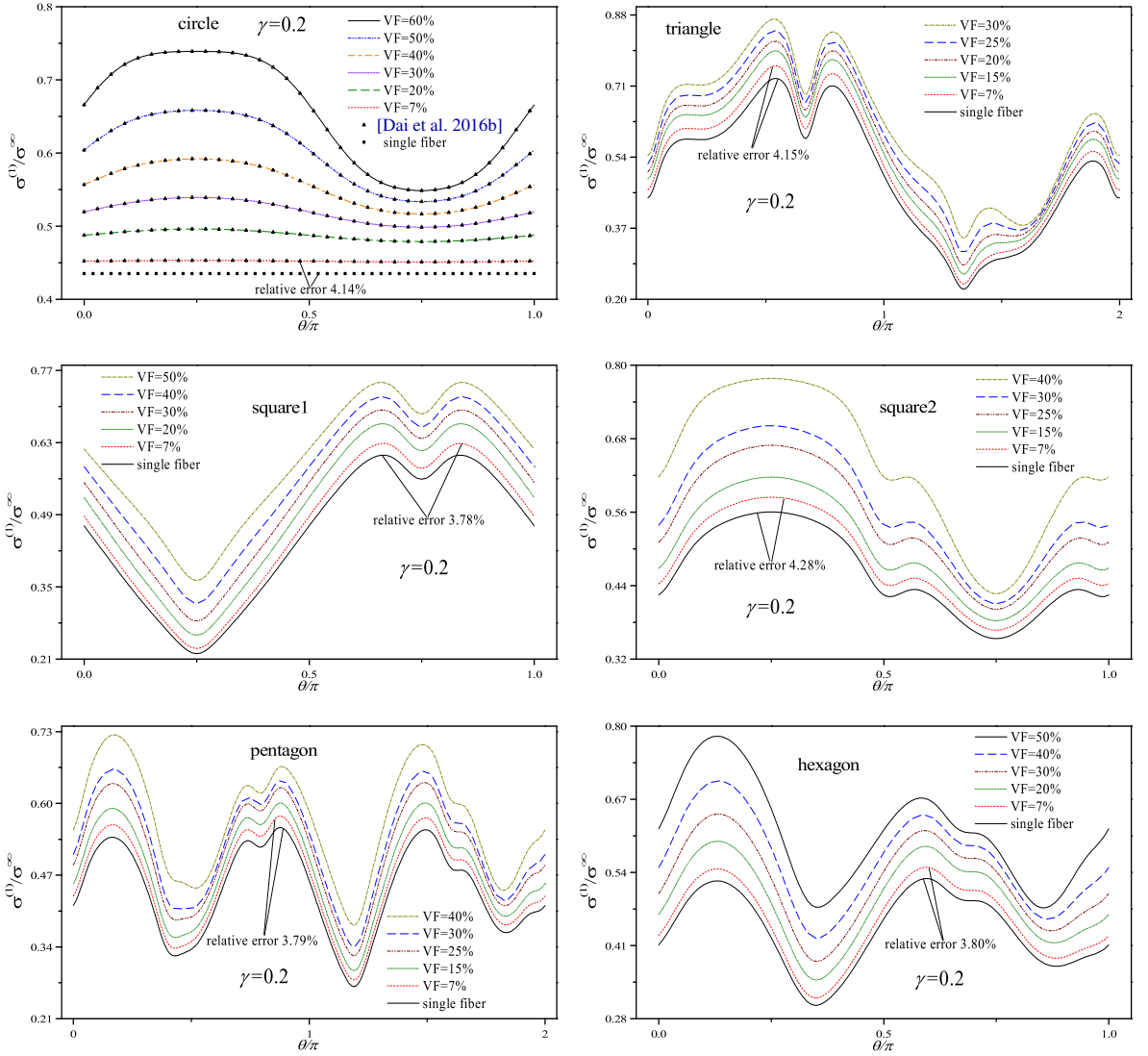


Figure 3. Resultant shear stresses around fiber on the interface between soft fiber and matrix. See caption on previous page for key.

moduli of the matrix and nanofibers [Tiersten 1969; Zhang et al. 2012]:

$$G_s = G_{s0} + G_{s1}, \quad (32)$$

where G_{s0} and G_{s1} are the surface moduli of the matrix and fibers, respectively. In particular, we simply assume $G_{s1}/G_{s0} = G_1/G_0$ since larger bulk moduli often indicate larger surface moduli. Consequently, the normalized interface parameter λ introduced from (12) is rewritten as

$$\lambda = \frac{G_{s0}(1 + \gamma)}{G_0 R} = \lambda_0(1 + \gamma), \quad \lambda_0 = \frac{G_{s0}}{G_0 R}, \quad (33)$$

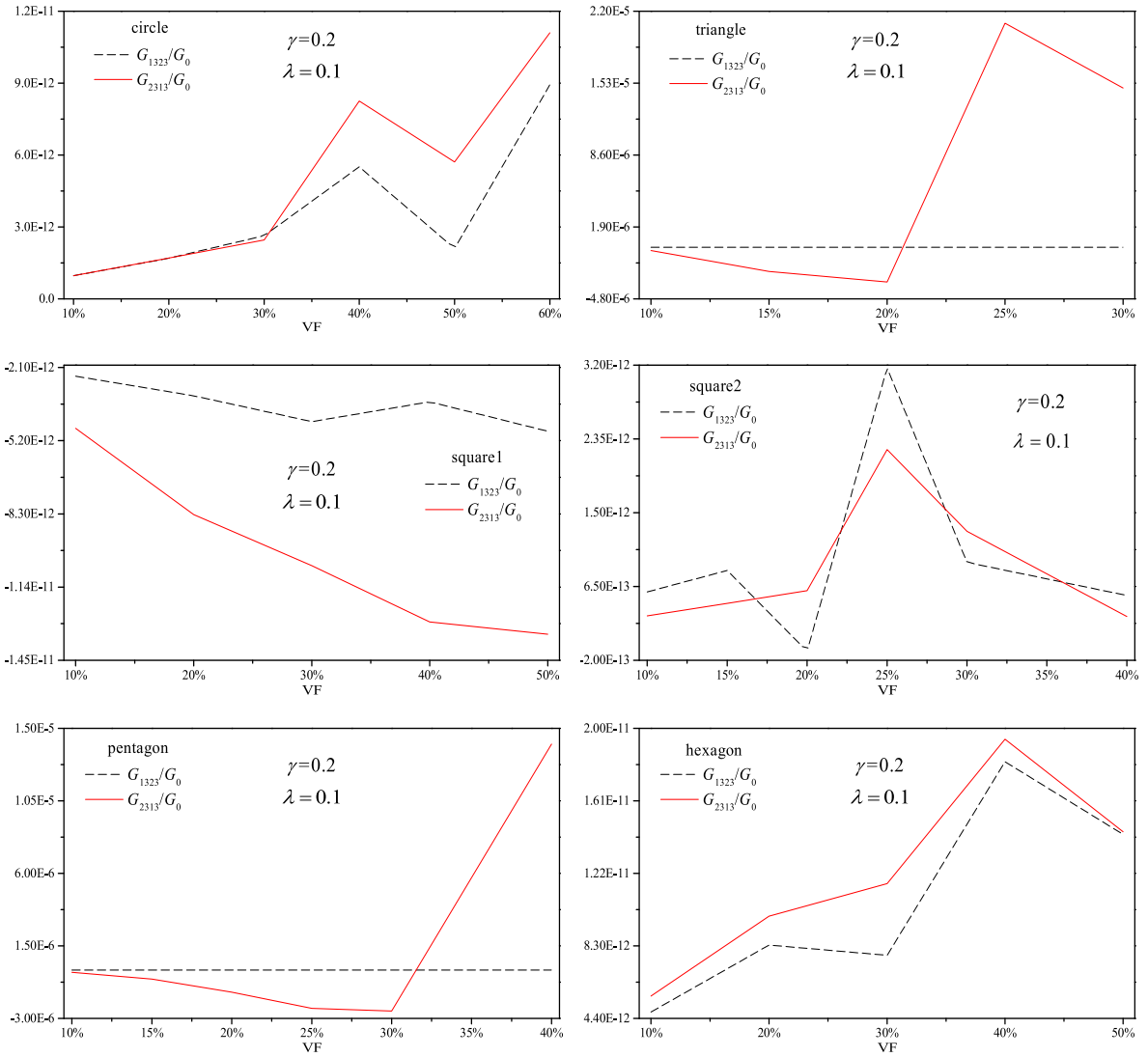


Figure 4. Minor effective longitudinal shear moduli of the composite with periodic soft fibers.

where λ_0 characterizes the normalized surface shear modulus of the matrix and it is taken as 0.1 in all of the following examples.

Figures 6–13 show the influence of the shape and volume fraction (VF) of the periodic fibers on the major effective (longitudinal) shear moduli G_{1313} and G_{2323} of the corresponding composite for several different interface parameters λ . In particular, G_{1313}^* and G_{2323}^* denote the specific major effective shear moduli of the composite when the interface effect is absent (or equivalently the interface parameter $\lambda = 0$). In Figures 7, 9, 11, and 13, we rearrange the results given respectively in Figures 6, 8, 10, and 12, and use the ratios G_{1313}/G_{1313}^* and G_{2323}/G_{2323}^* to demonstrate directly the contribution of interface effect to the major effective shear moduli of the composite with varying volume fraction of fibers.

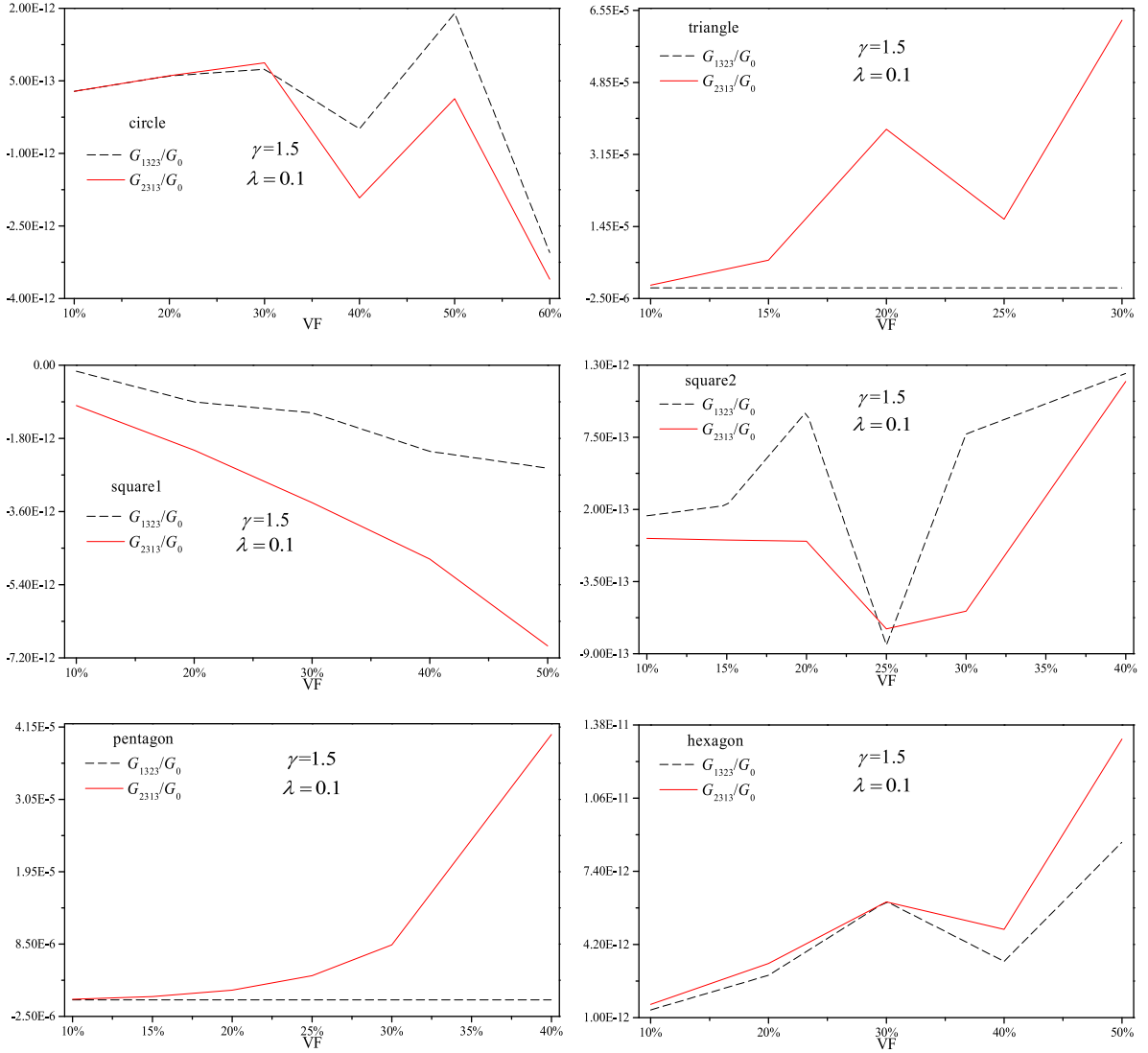


Figure 5. Minor effective longitudinal shear moduli of the composite with periodic hard fibers.

It is easily seen from Figures 6–13 that for a given fiber volume fraction, the major effective shear moduli of the composite containing periodic regular n -sided polygonal fibers decrease from the original increase with increasing n for the nonnegative value of λ when the fibers get harder. For the negative value of λ , the major effective shear moduli of the composite increase with increasing n . On the other hand, the contribution of the interface effect to the major effective shear moduli of this kind of composite decreases always with increasing n . These imply that for a given fiber volume fraction and interface parameter λ , the major effective shear moduli of the composite containing periodic circular fibers are larger but less sensitive to the interface effect as compared with those of the composites containing periodic regular polygonal fibers when the fibers are very soft. When the fibers get harder, the major effective shear moduli of the

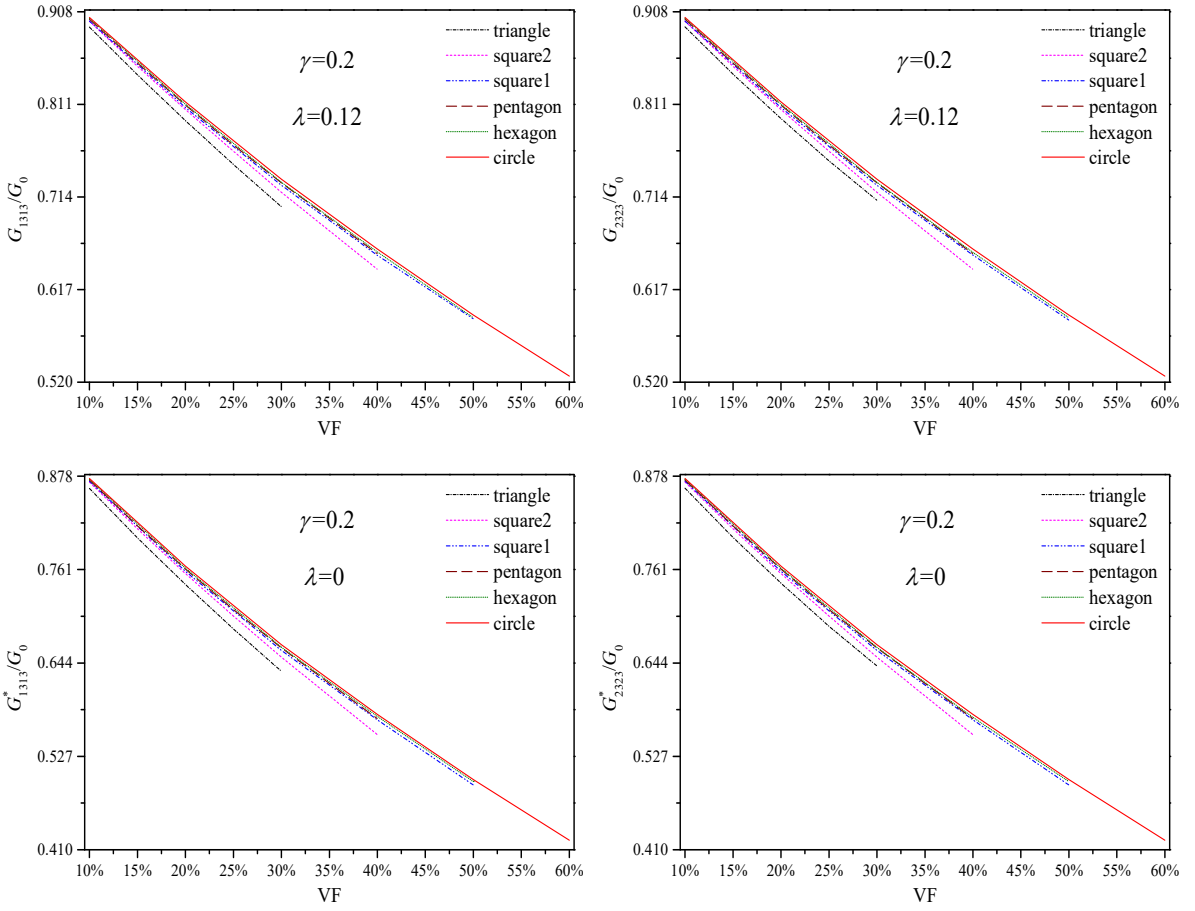


Figure 6. Major effective longitudinal shear moduli of the composite containing periodic soft fibers.

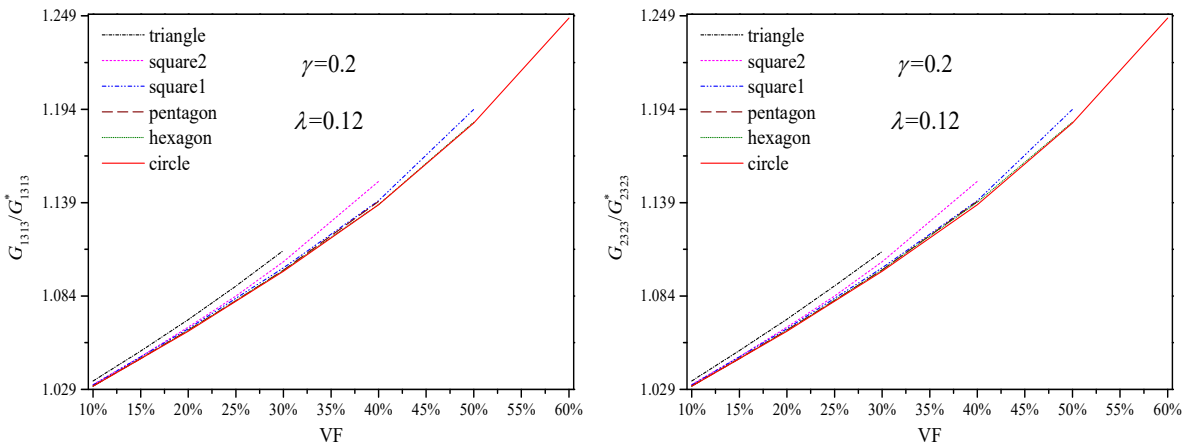


Figure 7. Contribution of interface effect to the major effective longitudinal shear moduli.

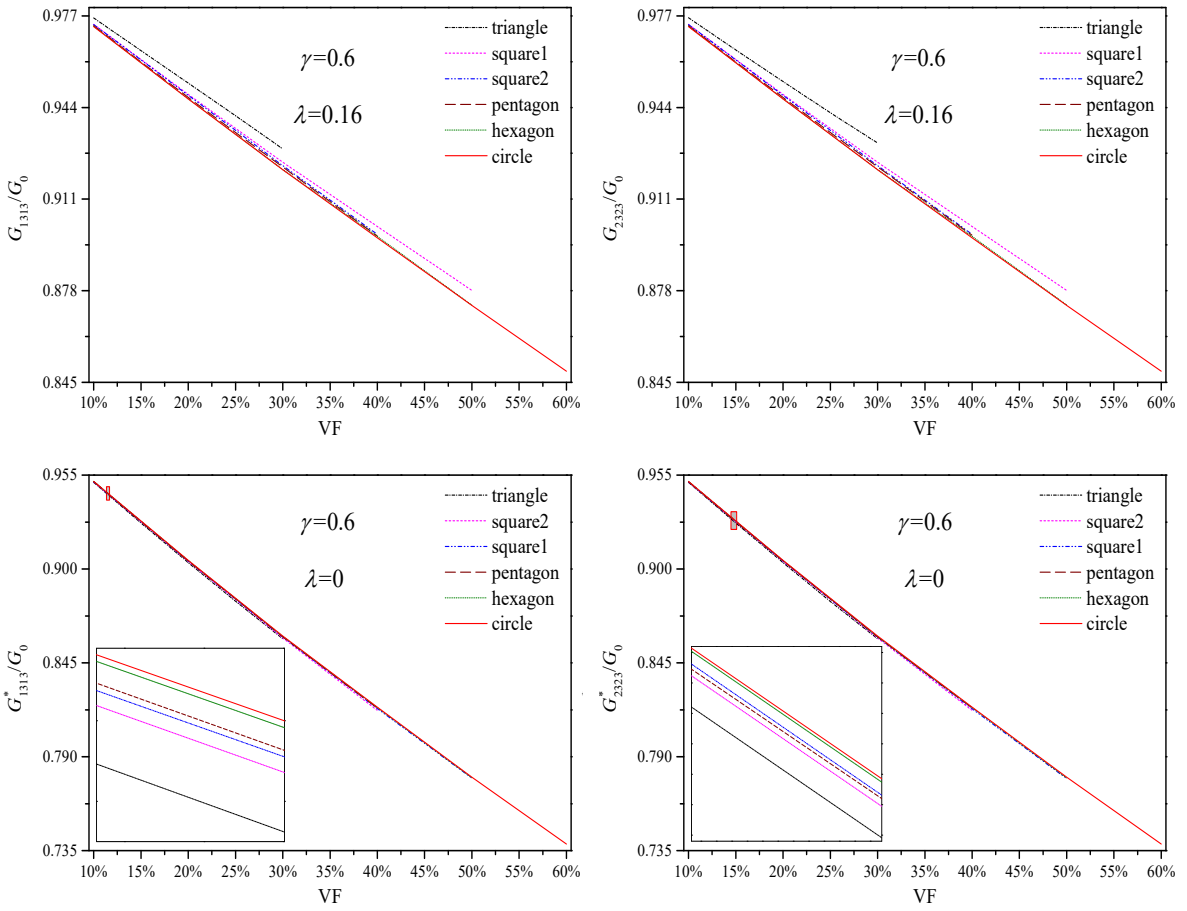


Figure 8. Major effective longitudinal shear moduli of the composite containing periodic soft fibers.

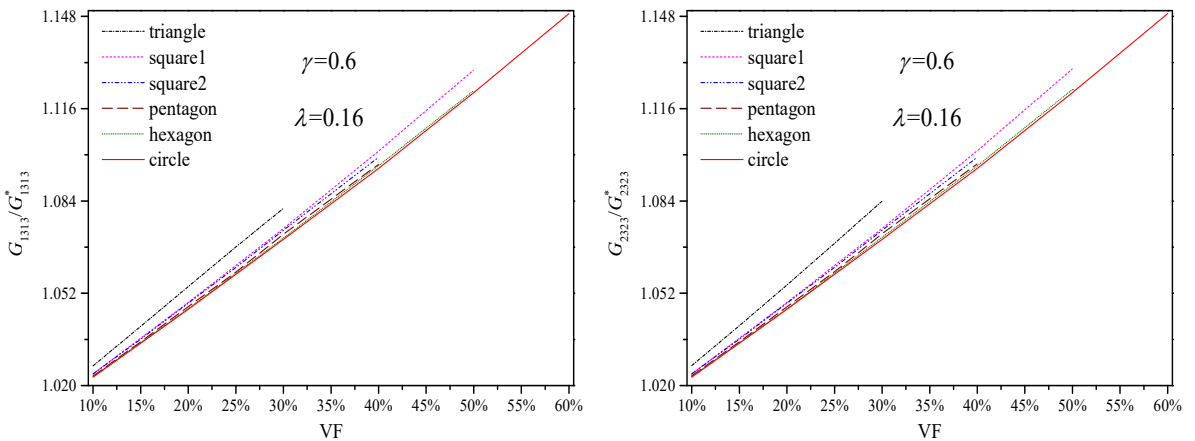


Figure 9. Contribution of interface effect to the major effective longitudinal shear moduli.

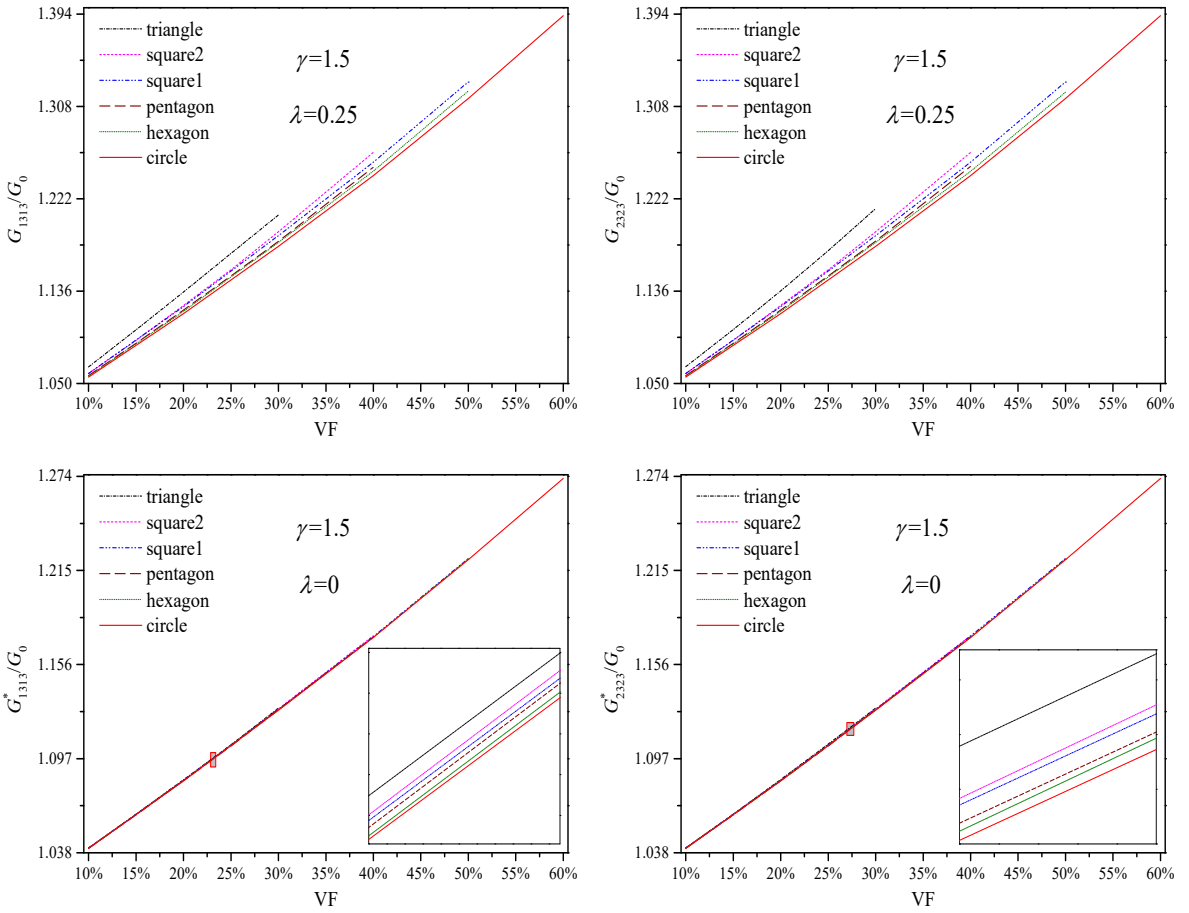


Figure 10. Major effective longitudinal shear moduli of the composite containing periodic hard fibers.

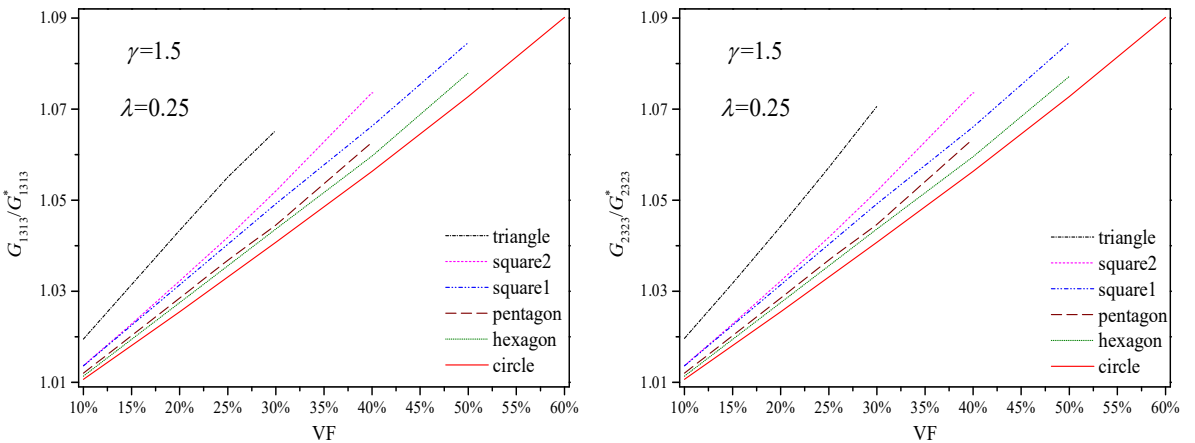


Figure 11. Contribution of interface effect to the major effective longitudinal shear moduli.

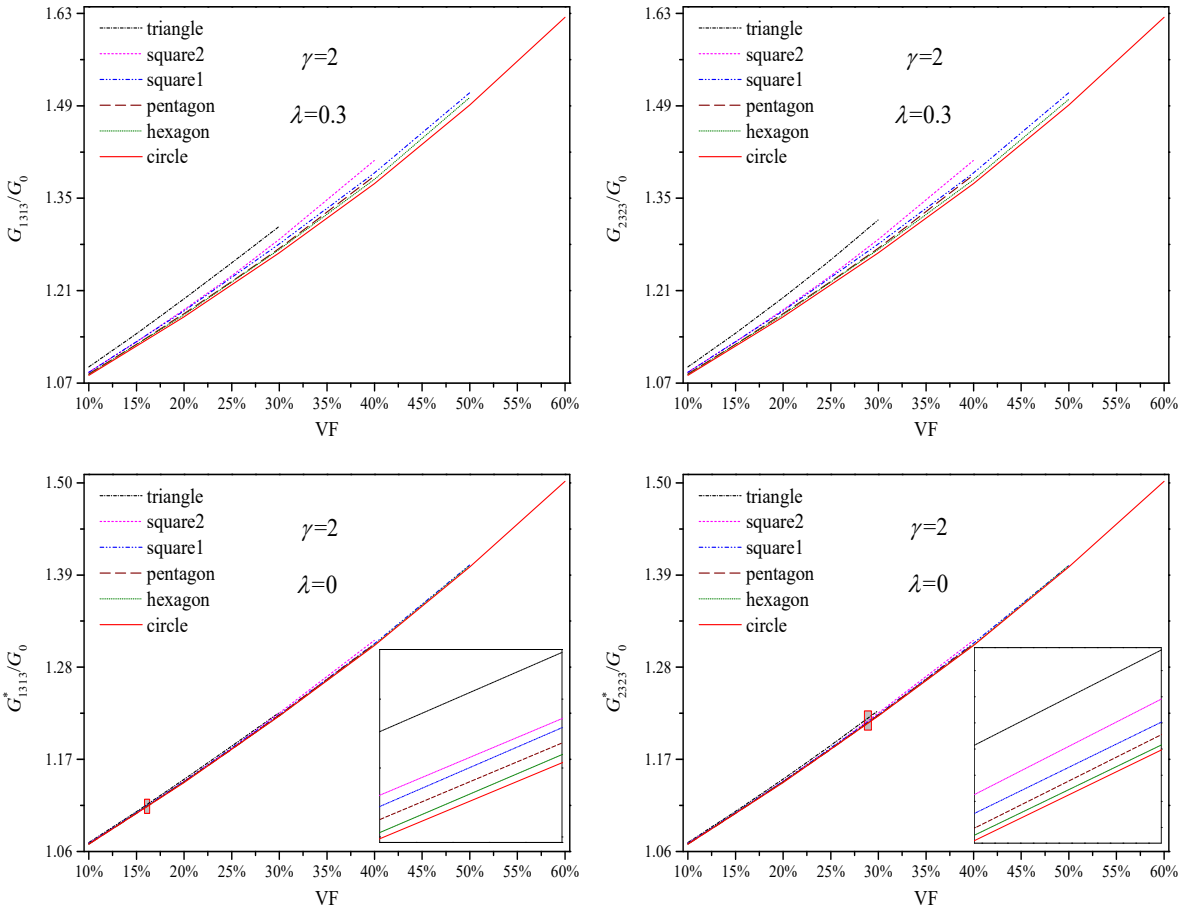


Figure 12. Major effective longitudinal shear moduli of the composite containing periodic hard fibers.

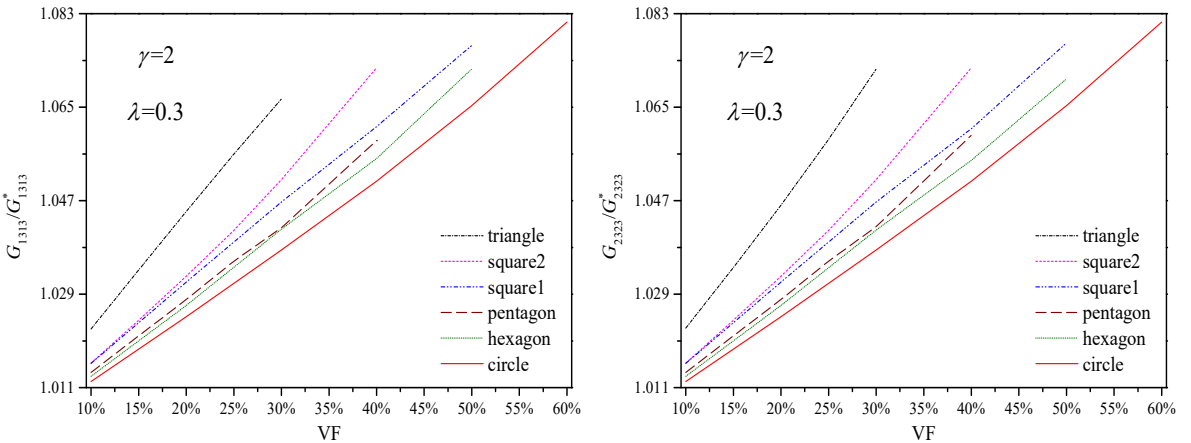


Figure 13. Contribution of interface effect to the major effective longitudinal shear moduli.

composite containing periodic circular fibers are still less sensitive to the interface effect but are smaller as compared with those of the composites containing periodic regular polygonal fibers. In addition, our results indicate that one can neglect the interface effect (i.e., treat the interfaces as being perfectly bonded to the matrix) when the shear modulus of the fibers reaches two (or more) times that of the matrix.

5. Conclusion

Based on the Gurtin–Murdoch model, the longitudinal shear behavior of composites with unidirectional periodic nanofibers of approximately regular polygonal shapes is investigated using a complex variable-based numerical procedure. Numerical results are presented for the stress concentration on the interfaces and the effective (longitudinal) shear moduli of the composite relative to the interface parameter, the volume fraction of the fibers, and the hardness of the fibers. The main findings are as follows:

- (1) The stress field around periodic fibers can be treated as that around a single fiber (of identical shape, size, and interface parameters) without inducing significant errors when the volume fraction of the periodic fibers is less than 7%.
- (2) For (reasonably) given interface parameters, fiber volume fraction and fiber size, the composite containing periodic circular fibers has the lowest sensitivity of effective shear moduli to the interface effect among all the composites containing periodic regular polygonal fibers.
- (3) The interface effect is negligible in the determination of the effective shear moduli of the composite when the shear modulus of the fibers reaches two (or more) times that of the matrix.

Acknowledgements

This project is supported by the National Natural Science Foundation of China (11472130 and 11232007) and a Project Funded by the Priority Academic Program Development of Jiangsu Higher Education Institutions (PAPD).

References

- [Chen et al. 2007] T. Chen, G. J. Dvorak, and C. C. Yu, “Size-dependent elastic properties of unidirectional nano-composites with interface stresses”, *Acta Mech.* **188** (2007), 39–54.
- [Dai et al. 2016a] M. Dai, L. C. Meng, C. Huang, and C. F. Gao, “Electro-elastic fields around two arbitrarily-shaped holes in a finite electrostrictive solid”, *Appl. Math. Model.* **40**:7-8 (2016), 4625–4639.
- [Dai et al. 2016b] M. Dai, P. Schiavone, and C. F. Gao, “Determination of effective thermal expansion coefficients of unidirectional fibrous nanocomposites”, *Zeitschrift für angewandte Mathematik und Physik* **67**:5 (2016), 110.
- [Dai et al. 2016c] M. Dai, P. Schiavone, and C. F. Gao, “Prediction of the stress field and effective shear modulus of composites containing periodic inclusions incorporating interface effects in anti-plane shear”, *J. Elasticity* **125**:2 (2016), 217–230.
- [Dai et al. 2016d] M. Dai, P. Schiavone, and C. F. Gao, “Uniqueness of neutral elastic circular nano-inhomogeneities in antiplane shear and plane deformations”, *J. Appl. Mech. (ASME)* **83**:10 (2016), 101001.
- [Dai et al. 2017] M. Dai, P. Schiavone, and C. F. Gao, “A new method for the evaluation of the effective properties of composites containing unidirectional periodic nanofibers”, *Arch. Appl. Mech.* **87**:4 (2017), 647–665.
- [Dai et al. 2018] M. Dai, A. Gharahi, and P. Schiavone, “Analytic solution for a circular nano-inhomogeneity with interface stretching and bending resistance in plane strain deformations”, *Appl. Math. Model.* **55** (2018), 160–170.
- [Duan et al. 2005] H. L. Duan, J. Wang, Z. P. Huang, and B. L. Karihaloo, “Size-dependent effective elastic constants of solids containing nano-inhomogeneities with interface stress”, *J. Mech. Phys. Solids* **53** (2005), 1574–1596.

- [Gurtin and Murdoch 1975] M. E. Gurtin and A. I. Murdoch, “A continuum theory of elastic material surfaces”, *Arch. Ration. Mech. Anal.* **57**:4 (1975), 291–323.
- [Gurtin and Murdoch 1978] M. E. Gurtin and A. I. Murdoch, “Surface stress in solids”, *Int. J. Solids Struct.* **14**:6 (1978), 431–440.
- [Gurtin et al. 1998] M. E. Gurtin, J. Weissmüller, and F. Larche, “A general theory of curved deformable interfaces in solids at equilibrium”, *Philos. Mag. A* **78**:5 (1998), 1093–1109.
- [Josell et al. 1999] D. Josell, J. E. Bonevich, I. Shao, and R. C. Cammarata, “Measuring the interface stress: silver/nickel interfaces”, *J. Mater. Res.* **14**:11 (1999), 4358–4365.
- [Lim et al. 2006] C. W. Lim, Z. R. Li, and L. H. He, “Size dependent, non-uniform elastic field inside a nano-scale spherical inclusion due to interface stress”, *Int. J. Solids Struct.* **43**:17 (2006), 5055–5065.
- [Luo and Wang 2009] J. Luo and X. Wang, “On the anti-plane shear of an elliptic nano inhomogeneity”, *Eur. J. Mech. A Solids* **28**:5 (2009), 926–934.
- [Mogilevskaya et al. 2008] S. G. Mogilevskaya, S. L. Crouch, and H. K. Stolarski, “Multiple interacting circular nano-inhomogeneities with surface/interface effects”, *J. Mech. Phys. Solids* **56** (2008), 2298–2327.
- [Mogilevskaya et al. 2010] S. G. Mogilevskaya, S. L. Crouch, H. K. Stolarski, and A. Benusioglio, “Equivalent inhomogeneity method for evaluating the effective elastic properties of unidirectional multi-phase composites with surface/interface effects”, *Int. J. Solids Struct.* **47**:3-4 (2010), 407–418.
- [Muskhelishvili 1975] N. I. Muskhelishvili, *Some basic problems of the mathematical theory of elasticity*, Noordhoff, Groningen, The Netherlands, 1975.
- [Ruud et al. 1993] J. A. Ruud, A. Witvrouw, and F. Spaepen, “Bulk and interface stresses in silver-nickel multilayered thin films”, *J. Appl. Phys.* **74**:4 (1993), 2517–2523.
- [Sharma et al. 2003] P. Sharma, S. Ganti, and N. Bhate, “Effect of surfaces on the size-dependent elastic state of nano-inhomogeneities”, *Appl. Phys. Lett.* **82**:4 (2003), 535–537.
- [Tian and Rajapakse 2007] L. Tian and R. Rajapakse, “Elastic field of an isotropic matrix with a nanoscale elliptical inhomogeneity”, *Int. J. Solids Struct.* **44**:24 (2007), 7988–8005.
- [Tiersten 1969] H. F. Tiersten, “Elastic surface waves guided by thin films”, *J. Appl. Phys.* **40** (1969), 770–789.
- [Wang and Schiavone 2014] X. Wang and P. Schiavone, “Interaction of a screw dislocation with a nano-sized, arbitrarily shaped inhomogeneity with interface stresses under anti-plane deformations”, *Proc. Royal Soc. A* **470**:2170 (2014), art. id. 20140313.
- [Xia et al. 2003] Z. H. Xia, Y. F. Zhang, and F. Ellyin, “A unified periodical boundary conditions for representative volume elements of composites and applications”, *Int. J. Solids Struct.* **40**:8 (2003), 1907–1921.
- [Yvonnet et al. 2008] J. Yvonnet, H. L. Quang, and Q. C. He, “An XFEM/level set approach to modelling surface/interface effects and to computing the size-dependent effective properties of nanocomposites”, *Comput. Mech.* **42** (2008), 119–131.
- [Zhang et al. 2012] C. Zhang, W. Chen, and C. Zhang, “On propagation of anti-plane shear waves in piezoelectric plates with surface effect”, *Phys. Lett. A* **376** (2012), 3281–3286.

Received 11 Sep 2017. Revised 23 Jan 2018. Accepted 14 Feb 2018.

HAI-BING YANG: yanghb@scut.edu.cn

Department of Mechanics Engineering, School of Civil Engineering and Transportation, South China University of Technology, Guangzhou, China

CHENG HUANG: hc_12345@nuaa.edu.cn

State Key Laboratory of Mechanics and Control of Mechanical Structures, Nanjing University of Aeronautics and Astronautics, Nanjing, China

CHUAN-BIN YU: cbyu@nuaa.edu.cn

State Key Laboratory of Mechanics and Control of Mechanical Structures, Nanjing University of Aeronautics and Astronautics, Nanjing, China

CUN-FA GAO: cfgao@nuaa.edu.cn

State Key Laboratory of Mechanics and Control of Mechanical Structures, Nanjing University of Aeronautics and Astronautics, Nanjing, China

JOURNAL OF MECHANICS OF MATERIALS AND STRUCTURES

msp.org/jomms

Founded by Charles R. Steele and Marie-Louise Steele

EDITORIAL BOARD

| | |
|-----------------------|--|
| ADAIR R. AGUIAR | University of São Paulo at São Carlos, Brazil |
| KATIA BERTOLDI | Harvard University, USA |
| DAVIDE BIGONI | University of Trento, Italy |
| MAENGHYO CHO | Seoul National University, Korea |
| HUILING DUAN | Beijing University |
| YIBIN FU | Keele University, UK |
| IWONA JASIUK | University of Illinois at Urbana-Champaign, USA |
| DENNIS KOCHMANN | ETH Zurich |
| MITSUTOSHI KURODA | Yamagata University, Japan |
| CHEE W. LIM | City University of Hong Kong |
| ZISHUN LIU | Xi'an Jiaotong University, China |
| THOMAS J. PENCE | Michigan State University, USA |
| GIANNI ROYER-CARFAGNI | Università degli studi di Parma, Italy |
| DAVID STEIGMANN | University of California at Berkeley, USA |
| PAUL STEINMANN | Friedrich-Alexander-Universität Erlangen-Nürnberg, Germany |
| KENJIRO TERADA | Tohoku University, Japan |

ADVISORY BOARD

| | |
|---------------|---|
| J. P. CARTER | University of Sydney, Australia |
| D. H. HODGES | Georgia Institute of Technology, USA |
| J. HUTCHINSON | Harvard University, USA |
| D. PAMPLONA | Universidade Católica do Rio de Janeiro, Brazil |
| M. B. RUBIN | Technion, Haifa, Israel |

PRODUCTION production@msp.org

SILVIO LEVY Scientific Editor


Cover photo: Mando Gomez, www.mandolux.com

See msp.org/jomms for submission guidelines.

JoMMS (ISSN 1559-3959) at Mathematical Sciences Publishers, 798 Evans Hall #6840, c/o University of California, Berkeley, CA 94720-3840, is published in 10 issues a year. The subscription price for 2018 is US \$615/year for the electronic version, and \$775/year (+\$60, if shipping outside the US) for print and electronic. Subscriptions, requests for back issues, and changes of address should be sent to MSP.

JoMMS peer-review and production is managed by EditFLOW® from Mathematical Sciences Publishers.

PUBLISHED BY

 **mathematical sciences publishers**
nonprofit scientific publishing

<http://msp.org/>

© 2018 Mathematical Sciences Publishers

Journal of Mechanics of Materials and Structures

Volume 13, No. 2

March 2018

- A simple technique for estimation of mixed mode (I/II) stress intensity factors**
SOMAN SAJITH, KONDEPUDI S.R.K. MURTHY and PUTHUVEETIL S. ROBI 141
- Longitudinal shear behavior of composites with unidirectional periodic nanofibers of some regular polygonal shapes**
HAI-BING YANG, CHENG HUANG, CHUAN-BIN YU and CUN-FA GAO 155
- Fracture initiation in a transversely isotropic solid: transient three dimensional analysis** LOUIS M. BROCK 171
- Eshelby inclusion of arbitrary shape in isotropic elastic materials with a parabolic boundary** XU WANG, LIANG CHEN and PETER SCHIAVONE 191
- Burmister's problem extended to a microstructured layer** THANASIS ZISIS 203
- Multiple crack damage detection of structures using simplified PZT model**
NARAYANAN JINESH and KRISHNAPILLAI SHANKAR 225